Hindawi
Advanced Gut & Microbiome Research
Volume 2022, Article ID 7883756, 13 pages
https://doi.org/10.1155/2022/7883756

Research Article

Network Pharmacology Analysis of Xuanfei Baidu Granule in the Treatment of Intestinal Flora Disorder

Yaodong Miao,[1,2] **Rui Chen**,[3] **Zeyu Zhang**,[4] **Yaoyuan Liu**,[4] **Fengwen Yang**,[5] **and Junhua Zhang**[6]

[1]*Second Affiliated Hospital of Tianjin University of Traditional Chinese Medicine, 300250 Tianjin, China*
[2]*State Key Laboratory of Component-Based Chinese, Tianjin University of Traditional Chinese Medicine, 301617 Tianjin, China*
[3]*School of Traditional Chinese Medicine, Tianjin University of Traditional Chinese Medicine, 301617 Tianjin, China*
[4]*First Teaching Hospital of Tianjin University of Traditional Chinese Medicine, National Clinical Research Center for Chinese Medicine Acupuncture and Moxibustion, Tianjin 300381, China*
[5]*Evidence-Based Medicine Center, Tianjin University of Traditional Chinese Medicine, Tianjin 301617, China*
[6]*Haihe Laboratory of Modern Chinese Medicine, Tianjin University of Traditional Chinese Medicine, Tianjin 301617, China*

Correspondence should be addressed to Fengwen Yang; 13682027022@163.com

Received 6 June 2022; Accepted 7 August 2022; Published 11 October 2022

Academic Editor: Jian Wu

Objective. This study is aimed at analyzing the molecular mechanism of Xuanfei Baidu Granule (XFBDG) in the treatment of intestinal flora disorder based on network pharmacology. *Methods*. The TCMSP database was used to obtain the active components and target proteins of XFBDG, while the GeneCards database was used to obtain the related proteins of intestinal flora disorder. The Rx64 4.0.2 software was used to analyze the GO functional enrichment and KEGG pathway enrichment of drug component target protein and disease-related protein to obtain the pathway-enriched proteins and screen the core proteins for topology analysis of the pathway target by using the STRING database and Cytoscape v3.8.2 software. The Cytoscape v3.8.2 software was used to analyze the relationship between each component and enriched protein, and the AutoDock Vina software was used for molecular docking of core proteins and components. *Results*. XFBDG contains 133 active components that can act on 249 proteins related to intestinal flora disorder. The effects include the following: (i) regulation of functions—the response to drug, cellular response to chemical stress, response to oxidative stress, and RNA polymerase II-specific DNA-binding transcription factor binding and (ii) regulation of signaling pathways such as the IL-17 signaling pathway, TNF signaling pathway, and Th17 cell differentiation pathway. The enriched core proteins in these pathways are IFNG, IL4, PTGS2, JUN, and IL1B that set in a higher level of binding with the corresponding drug components. *Conclusion*. XFBDG can act on IFNG, IL4, PTGS2, JUN, and IL1B proteins through its active components such as quercetin, luteolin, and kaempferol to regulate the IL-17, TNF, and Th17 cell differentiation pathways and further regulate the response to drug, cellular response to chemical stress, response to oxidative stress, and RNA polymerase II-specific DNA-binding transcription factor binding. In addition, owing to its antioxidant and anti-inflammatory properties and related immune responses, XFBDG can achieve a balance of intestinal flora and microbial metabolism.

1. Introduction

Xuanfei Baidu Granule (XFBDG) is an effective prescription developed by academician Zhang Boli to cope with the coronavirus disease 2019 (COVID-19) pandemic, which has been entered into the "The Diagnosis and Treatment Program of Coronavirus Pneumonia (A Trial Version of the Sixth and Seventh Edition)." Its prescription includes the classic prescription of traditional Chinese medicine (TCM) ingredients including Maxingshigan Decoction (MXSGD), Maxingyigan Decoction (MXYGD), Tinglidazao Xiefei Decoction (TLDZXFD), and Qianjin Weijing Decoction (QJWJD). XFBDG can ventilate the lung to eliminate dampness, clear heat for expelling pathogenic factors from the

exterior, remove heat from the lung, and carry out overall detoxification. The most important function of XFBDG is to treat the symptoms of stagnated lungs due to noxious dampness; accordingly, it has been widely used with a significant curative effect as a first-line COVID-19 therapy. The classic theory of TCM states that "the lungs are associated with the large intestine which is mainly in charge of transportation." Furthermore, "the lungs and the large intestine are intertwined in a mutual relationship," which means that both organs interact with and are influenced by each other, both physiologically and pathologically. Intestinal microbes and their metabolites are closely related to human health, and this is consistent with the recognition of modern medicine on the relationship between intestinal microbes and respiratory diseases. Therefore, maintaining intestinal microbial homeostasis has great significance for the prevention and treatment of pulmonary diseases: (i) microecological experiments have proven that some flora can change synchronously in the pulmonary or intestinal diseases of rats, which indicate that the change of microecological flora could be one of the ways and manifestations of "pulmonary and intestinal diseases" [1], (ii) modern medicine believes that various respiratory diseases can be prevented by regulating intestinal flora and intestinal immunity, suggesting that the gut-lung axis could be the bridge between the lung and large intestine [2–4], (iii) MXSGD can regulate Th1/Th2 immune balance, increase the numbers of *Bifidobacteria* and *Lactobacillus*, improve intestinal flora, and relieve clinical symptoms of bronchial asthma [5], (iv) MXSGD combined with azithromycin also has noticeable efficacy in the treatment of mycoplasma pneumonia for children, which can relate to the improvement of immune function by increasing anti-inflammatory factors and decreasing proinflammatory factors [6], and (v) QJWJD has similar immune effects on the decomposition of intestinal flora and filamentous bacteria, both of which can be affected by the expression of Th17 cell genes and proteins [7, 8].

Network pharmacology has become a new strategy for drug research, as it can accurately predict and analyze the mechanism of action of TCM compounds by interpreting the regulation mechanism of drugs on diseases from micro to macrodimensions. In addition, molecular docking can calculate the affinity between the receptor and ligand and some forms of binding, by which the results can be evaluated and screened. Given the efficacy of the classic prescription combined to formulate XFBDG for the treatment of intestinal flora disorder, this study adopts network pharmacology to explore the molecular mechanism of the prescription in the treatment of intestinal flora disorder, aiming to provide clues and ideas for subsequent experiments and clinical research.

2. Data and Methods

2.1. Ingredient Screening and Target Protein Acquisition. The following were considered as the conditions from the TCMSP database (http://tcmspw.com/tcmsp.php) to screen the effective components and target proteins of XFBDG (except gypsum): oral bioavailability (OB) ≥ 30%, drug − likeness (DL) ≥ 0.18, octanol − water partition coefficient (logP) ≤ 5, hydrogen bond donors (hdon) ≤ 5, hydrogen bond acceptors (HACC) ≤ 10, and relative molecular weight (MW) < 500 [9, 10]. The main component CaSO4 target protein of gypsum was screened from the SEA database (https://sea.bkslab.org/), and the last step was to import all target proteins into the UniProt database (https://www.uniprot.org/) for standardization of their names.

2.2. Intersection Targets of Acquisition of "Disease-Related Protein" and "Effective Component Target Protein." "Intestinal flora disorder", "Dysbiosis of the intestinal flora," and "Intestinal dysbiosis" were selected as the search term from the GeneCards database (http://www.genecards.org/) to obtain the disease-related proteins and void intersection with target protein of XFBDG, which was finally saved as a file and named *Drug-Disease*.

2.3. Analysis of GO Functional Enrichment and KEGG Pathway Enrichment. Drug-Disease was analyzed using the Rx64 4.0.2 software with $P < 0.05$ as the screening condition for GO functional enrichment analysis and KEGG pathway enrichment analysis. GO functional enrichment analysis mainly includes biological process (BP), molecular function (MF), and cellular component (CC). The top 10 functions of each of the three sections obtained through GO enrichment analysis are presented as bar charts, while the first 30 pathways obtained through KEGG pathway enrichment analysis are presented as bubble maps (the ordinate is the pathway name, the abscissa is the gene proportion, the circle area represents the number of enriched genes, and the color represents the enrichment degree, with darker red representing more noticeable enrichment). A literature search about disease-related pathways was carried out using PubMed (https://pubmed.ncbi.nlm.nih.gov/), and data on enriched proteins were obtained from the KEGG enrichment results. The STRING database and Cytoscape v3.8.2 software were used to screen the enriched core proteins and to make path-target topology analysis on the conditions that the degree value, degree of mediator, density, centrality, and the local-edged connectivity of network were all higher than the median level.

2.4. Network Construction of a Component-Target Topology Analysis. The active components and pathway-enriched proteins of XFBDG were imported into the Cytoscape v3.8.2 software and then processed in the visualization method to construct the component-target network in which the node represents compounds and targets and the line represents the interaction relationship between nodes.

2.5. Molecular Docking Verification and Screening. In molecular docking, the enriched core protein was used as the receptor, while the corresponding TCM component was used as the ligand. The 2D structure of TCM components was transformed into the 3D structure with the Chem3D.exe software, and its structure was optimized and saved as lig.mol2. The crystal structure of the target protein was obtained through the PDB database (http://www.rcsb.org/), and it was treated by PyMolwin.exe software to remove H_2O and small molecule ligands and saved as rep.pdb. The

Table 1: Effective components of XFBDG.

MOL ID	Name	MW	AlogP	Hdon	Hacc	OB	DL	Drug
MOL010788	Leucopelargonidin	290.29	1.36	5	6	57.97	0.24	Ephedra
MOL002823	Herbacetin	302.25	1.5	5	7	36.07	0.27	Ephedra
MOL000422	Kaempferol	286.25	1.77	4	6	41.88	0.24	Ephedra/root of Ural licorice/European verbena herb/sweet wormwood herb/Lepidium seed
MOL000098	Quercetin	302.25	1.5	5	7	46.43	0.28	Ephedra/root of Ural licorice/European verbena herb/sweet wormwood herb/Lepidium seed/patchouli/ Polygonum cuspidatum
MOL000006	Luteolin	286.25	2.07	4	6	36.16	0.25	Ephedra/European verbena herb/sweet wormwood herb/Polygonum cuspidatum
MOL000492	(+)-Catechin	290.29	1.92	5	6	54.83	0.24	Ephedra/Polygonum cuspidatum/bitter apricot seed
MOL002881	Diosmetin	300.28	2.32	3	6	31.14	0.27	Ephedra/European verbena herb
MOL004328	Naringenin	272.27	2.3	3	5	59.29	0.21	Ephedra/root of Ural licorice/ Pummelo Peel
MOL004576	Taxifolin	304.27	1.49	5	7	57.84	0.27	Ephedra
MOL005190	Eriodictyol	288.27	2.03	4	6	71.79	0.24	Ephedra
MOL005573	Genkwanin	284.28	2.59	2	5	37.13	0.24	Ephedra/patchouli
MOL005842	Pectolinarigenin	314.31	2.57	2	6	41.17	0.3	Ephedra
MOL004841	Licochalcone B	286.3	2.88	3	5	76.76	0.19	Root of Ural licorice/bitter apricot seed
MOL007207	Machiline	285.37	2.83	3	4	79.64	0.24	Bitter apricot seed
MOL010921	Estrone	270.4	3.77	1	2	53.56	0.32	Bitter apricot seed
MOL004908	Glabridin	324.4	3.95	2	4	53.25	0.47	Root of Ural licorice/bitter apricot seed
MOL012922	l-SPD	327.41	3.1	2	5	87.35	0.54	Bitter apricot seed
MOL005017	Phaseol	336.36	4.87	2	5	78.77	0.58	Bitter apricot seed
MOL002311	Glycyrol	366.39	4.85	2	6	90.78	0.67	Bitter apricot seed
MOL004903	Liquiritin	418.43	0.66	5	9	65.69	0.74	Root of Ural licorice/bitter apricot seed
MOL001323	Sitosterol alpha1	426.8	8.15	1	1	43.28	0.78	Seed of Job's tears
MOL001494	Mandenol	308.56	6.99	0	2	42	0.19	Seed of Job's tears
MOL000359	Sitosterol	414.79	8.08	1	1	36.91	0.75	Seed of Job's tears
MOL000449	Stigmasterol	412.77	7.64	1	1	43.83	0.76	Seed of Job's tears/reed rhizome
MOL000953	CLR	386.73	7.38	1	1	37.87	0.68	Seed of Job's tears
MOL000173	Wogonin	284.28	2.59	2	5	30.68	0.23	Rhizoma Atractylodis
MOL000188	3β-Acetoxyatractylone	274.39	3.39	0	3	40.57	0.22	Rhizoma Atractylodis
MOL005911	5-Hydroxy-7,4′-dimethoxyflavanon	300.33	2.8	1	5	51.54	0.27	Patchouli
MOL005916	Irisolidone	314.31	2.3	2	6	37.78	0.3	Patchouli
MOL005918	Phenanthrone	293.34	4.27	0	3	38.7	0.33	Patchouli
MOL005921	Quercetin 7-O-β-D-glucoside	300.28	2.17	5	6	49.57	0.27	Patchouli
MOL002235	Eupatin	360.34	1.99	3	8	50.8	0.41	Sweet wormwood herb
MOL000354	Isorhamnetin	316.28	1.76	4	7	49.6	0.31	Root of Ural licorice/sweet wormwood herb/Lepidium seed
MOL004083	Tamarixetin	316.28	1.76	4	7	32.86	0.31	Sweet wormwood herb
MOL004112	Patuletin	332.28	1.49	5	8	53.11	0.34	Sweet wormwood herb
MOL004609	Areapillin	360.34	2.29	3	8	48.96	0.41	Sweet wormwood herb
MOL005229	Artemetin	388.4	2.31	1	8	49.55	0.48	Sweet wormwood herb/European verbena herb

Table 1: Continued.

MOL ID	Name	MW	AlogP	Hdon	Hacc	OB	DL	Drug
MOL007274	Skrofulein	314.31	2.57	2	6	30.35	0.3	Sweet wormwood herb
MOL007401	Cirsiliol	330.31	2.3	3	7	43.46	0.34	Sweet wormwood herb
MOL007404	vitexin_qt	270.25	1.17	3	5	52.18	0.21	Sweet wormwood herb
MOL007412	DMQT	346.31	1.55	4	8	42.6	0.37	Sweet wormwood herb
MOL007415	[(2S)-2-[[(2S)-2-(Benzoylamino) -3-phenylpropanoyl]amino] -3-phenylpropyl] acetate	444.57	4.02	2	6	58.02	0.52	Sweet wormwood herb
MOL007423	6,8-di-c-Glucosylapigenin_qt	270.25	1.17	3	5	59.85	0.21	Sweet wormwood herb
MOL007424	Artemisinin	282.37	3.14	0	5	49.88	0.31	Sweet wormwood herb
MOL007426	Deoxyartemisinin	266.37	2.15	0	4	54.47	0.26	Sweet wormwood herb
MOL013281	6,8-Dihydroxy-7-methoxyxanthone	258.24	2.41	2	5	35.83	0.21	Polygonum cuspidatum
MOL013287	Physovenine	262.34	2.08	1	5	106.21	0.19	Polygonum cuspidatum
MOL013288	Picralinal	366.45	1.8	1	6	58.01	0.75	Polygonum cuspidatum
MOL002268	Rhein	284.23	1.88	3	6	47.07	0.28	Polygonum cuspidatum
MOL002933	5,7,4′-Trihydroxy-8 -methoxyflavone	300.28	2.32	3	6	36.56	0.27	European verbena herb
MOL005503	Cornudentanone	378.56	4.97	0	5	39.66	0.33	European verbena herb
MOL008752	Dihydroverticillatine	423.55	3.98	2	6	42.69	0.84	European verbena herb
MOL003906	K-strophanthoside_qt	404.55	1.34	3	6	30.8	0.78	Lepidium seed
MOL003908	Cynotoxin	404.55	1.34	3	6	99.94	0.78	Lepidium seed
MOL013277	Isosinensetin	372.4	3.06	0	7	51.15	0.44	Pummelo Peel
MOL013279	5,7,4′-Trimethylapigenin	312.34	3.09	0	5	39.83	0.3	Pummelo Peel
MOL001798	neohesperidin_qt	302.3	2.28	3	6	71.17	0.27	Pummelo Peel
MOL001803	Sinensetin	372.4	3.06	0	7	50.56	0.45	Pummelo Peel
MOL005828	Nobiletin	402.43	3.04	0	8	61.67	0.52	Pummelo Peel
MOL005849	Didymin	286.3	2.55	2	5	38.55	0.24	Pummelo Peel
MOL001484	Inermine	284.28	2.44	1	5	75.18	0.54	Root of Ural licorice
MOL001792	DFV	256.27	2.57	2	4	32.76	0.18	Root of Ural licorice
MOL000239	Jaranol	314.31	2.09	2	6	50.83	0.29	Root of Ural licorice
MOL002565	Medicarpin	270.3	2.66	1	4	49.22	0.34	Root of Ural licorice
MOL003656	Lupiwighteone	338.38	3.92	3	5	51.64	0.37	Root of Ural licorice
MOL003896	7-Methoxy-2-methyl isoflavone	266.31	3.36	0	3	42.56	0.2	Root of Ural licorice
MOL000392	Formononetin	268.28	2.58	1	4	69.67	0.21	Root of Ural licorice
MOL000417	Calycosin	284.28	2.32	2	5	47.75	0.24	Root of Ural licorice
MOL004808	Glyasperin B	370.43	4.02	3	6	65.22	0.44	Root of Ural licorice
MOL004810	Glyasperin F	354.38	2.97	3	6	75.84	0.54	Root of Ural licorice
MOL004811	Glyasperin C	356.45	4.73	3	5	45.56	0.4	Root of Ural licorice
MOL004814	Isotrifoliol	298.26	2.99	2	6	31.94	0.42	Root of Ural licorice
MOL004815	(E)-1-(2,4-Dihydroxyphenyl) -3-(2,2-dimethylchromen -6-yl)prop-2-en-1-one	322.38	3.96	2	4	39.62	0.35	Root of Ural licorice
MOL004820	Kanzonol W	336.36	3.63	2	5	50.48	0.52	Root of Ural licorice
MOL004824	(2S)-6-(2,4-Dihydroxyphenyl) -2-(2-hydroxypropan-2-yl) -4-methoxy-2,3-dihydrofuro[3,2 -g]chromen-7-one	384.41	2.96	3	7	60.25	0.63	Root of Ural licorice
MOL004827	Semilicoisoflavone B	352.36	2.85	3	6	48.78	0.55	Root of Ural licorice
MOL004828	Glepidotin A	338.38	3.9	3	5	44.72	0.35	Root of Ural licorice
MOL004829	Glepidotin B	340.4	3.88	3	5	64.46	0.34	Root of Ural licorice
MOL004833	Phaseolinisoflavan	324.4	3.95	2	4	32.01	0.45	Root of Ural licorice

Table 1: Continued.

MOL ID	Name	MW	AlogP	Hdon	Hacc	OB	DL	Drug
MOL004835	Glypallichalcone	284.33	3.4	1	4	61.6	0.19	Root of Ural licorice
MOL004838	8-(6-Hydroxy-2-benzofuranyl) -2,2-dimethyl-5-chromenol	308.35	4.2	2	4	58.44	0.38	Root of Ural licorice
MOL004848	Licochalcone G	354.43	4.35	3	5	49.25	0.32	Root of Ural licorice
MOL004849	3-(2,4-Dihydroxyphenyl)-8 -(1,1-dimethylprop-2-enyl)-7 -hydroxy-5-methoxy-coumarin	368.41	4.03	3	6	59.62	0.43	Root of Ural licorice
MOL004855	Licoricone	382.44	4.16	2	6	63.58	0.47	Root of Ural licorice
MOL004856	Gancaonin A	352.41	4.17	2	5	51.08	0.4	Root of Ural licorice
MOL004857	Gancaonin B	368.41	3.91	3	6	48.79	0.45	Root of Ural licorice
MOL004863	3-(3,4-Dihydroxyphenyl)-5,7 -dihydroxy-8-(3-methylbut-2 -enyl)chromone	354.38	3.65	4	6	66.37	0.41	Root of Ural licorice
MOL004864	5,7-Dihydroxy-3 -(4-methoxyphenyl)-8 -(3-methylbut-2-enyl)chromone	352.41	4.17	2	5	30.49	0.41	Root of Ural licorice
MOL004866	2-(3,4-Dihydroxyphenyl) -5,7-dihydroxy-6-(3-methylbut -2-enyl)chromone	354.38	3.92	4	6	44.15	0.41	Root of Ural licorice
MOL004879	Glycyrin	382.44	4.67	2	6	52.61	0.47	Root of Ural licorice
MOL004882	Licocoumarone	340.4	4.98	3	5	33.21	0.36	Root of Ural licorice
MOL004883	Licoisoflavone	354.38	3.65	4	6	41.61	0.42	Root of Ural licorice
MOL004884	Licoisoflavone B	352.36	2.85	3	6	38.93	0.55	Root of Ural licorice
MOL004885	Licoisoflavanone	354.38	2.97	3	6	52.47	0.54	Root of Ural licorice
MOL004891	Shinpterocarpin	322.38	3.46	1	4	80.3	0.73	Root of Ural licorice
MOL004898	(E)-3-[3,4-Dihydroxy-5 -(3-methylbut-2-enyl)phenyl] -1-(2,4-dihydroxyphenyl)prop -2-en-1-one	340.4	4.49	4	5	46.27	0.31	Root of Ural licorice
MOL004904	Licopyranocoumarin	384.41	3.04	3	7	80.36	0.65	Root of Ural licorice
MOL004907	Glyzaglabrin	298.26	2.1	2	6	61.07	0.35	Root of Ural licorice
MOL004910	Glabranin	324.4	4.42	2	4	52.9	0.31	Root of Ural licorice
MOL004911	Glabrene	322.38	3.77	2	4	46.27	0.44	Root of Ural licorice
MOL004912	Glabrone	336.36	3.12	2	5	52.51	0.5	Root of Ural licorice
MOL004913	1,3-Dihydroxy-9-methoxy-6-benzofurano[3,2-c]chromenone	298.26	2.99	2	6	48.14	0.43	Root of Ural licorice
MOL004914	1,3-Dihydroxy-8,9-dimethoxy-6-benzofurano[3,2-c]chromenone	328.29	2.98	2	7	62.9	0.53	Root of Ural licorice
MOL004915	Eurycarpin A	338.38	3.92	3	5	43.28	0.37	Root of Ural licorice
MOL004924	(-)-Medicocarpin	432.46	0.75	4	9	40.99	0.95	Root of Ural licorice
MOL004935	Sigmoidin-B	356.4	3.89	4	6	34.88	0.41	Root of Ural licorice
MOL004941	(2R)-7-Hydroxy-2 -(4-hydroxyphenyl)chroman -4-one	256.27	2.57	2	4	71.12	0.18	Root of Ural licorice
MOL004945	(2S)-7-Hydroxy-2 -(4-hydroxyphenyl)-8 -(3-methylbut-2-enyl)chroman -4-one	324.4	4.42	2	4	36.57	0.32	Root of Ural licorice
MOL004948	Isoglycyrol	366.39	4.36	1	6	44.7	0.84	Root of Ural licorice
MOL004949	Isolicoflavonol	354.38	3.63	4	6	45.17	0.42	Root of Ural licorice
MOL004957	HMO	268.28	2.58	1	4	38.37	0.21	Root of Ural licorice
MOL004959	1-Methoxyphaseollidin	354.43	4.25	2	5	69.98	0.64	Root of Ural licorice

Table 1: Continued.

MOL ID	Name	MW	AlogP	Hdon	Hacc	OB	DL	Drug
MOL004961	Quercetin der.	330.31	1.82	3	7	46.45	0.33	Root of Ural licorice
MOL004966	3′–Hydroxy-4′-O-methylglabridin	354.43	3.93	2	5	43.71	0.57	Root of Ural licorice
MOL000497	Licochalcone A	338.43	4.62	2	4	40.79	0.29	Root of Ural licorice
MOL004974	3′-Methoxyglabridin	354.43	3.93	2	5	46.16	0.57	Root of Ural licorice
MOL004978	2-[(3R)-8,8-Dimethyl-3,4 -dihydro-2H-pyrano[6,5 -f]chromen-3-yl]-5-methoxyphenol	338.43	4.2	1	4	36.21	0.52	Root of Ural licorice
MOL004980	Inflacoumarin A	322.38	4.7	2	4	39.71	0.33	Root of Ural licorice
MOL004989	6-Prenylated eriodictyol	356.4	3.89	4	6	39.22	0.41	Root of Ural licorice
MOL004990	7,2′,4′-Trihydroxy-5-methoxy -3-arylcoumarin	300.28	2.56	3	6	83.71	0.27	Root of Ural licorice
MOL004991	7-Acetoxy-2-methylisoflavone	294.32	3.15	0	4	38.92	0.26	Root of Ural licorice
MOL004993	8-Prenylated eriodictyol	356.4	3.89	4	6	53.79	0.4	Root of Ural licorice
MOL000500	Vestitol	272.32	3.15	2	4	74.66	0.21	Root of Ural licorice
MOL005000	Gancaonin G	352.41	4.17	2	5	60.44	0.39	Root of Ural licorice
MOL005001	Gancaonin H	420.49	4.71	3	6	50.1	0.78	Root of Ural licorice
MOL005003	Licoagrocarpin	338.43	4.51	1	4	58.81	0.58	Root of Ural licorice
MOL005007	Glyasperin M	368.41	3.22	2	6	72.67	0.59	Root of Ural licorice
MOL005008	Glycyrrhiza flavonol A	370.38	2.17	4	7	41.28	0.6	Root of Ural licorice
MOL005012	Licoagroisoflavone	336.36	3.48	2	5	57.28	0.49	Root of Ural licorice
MOL005016	Odoratin	314.31	2.3	2	6	49.95	0.3	Root of Ural licorice
MOL005018	Xambioona	388.49	4.68	0	4	54.85	0.87	Root of Ural licorice
MOL005020	Dehydroglyasperin C	340.4	4.3	4	5	53.82	0.37	Root of Ural licorice

two files of rep.pdb and lig.mol2 were imported into AutoDockTools 1.5.6 software and transformed into PDBQT format to fix the active position. As Autodock Vina was used for molecular docking to select the components that have the lowest docking affinity with the target protein, PyMOLWin.exe software was used to visualize the docking results.

3. Results and Analysis

3.1. Effective Component and Target Protein of XFBDG. There are 132 kinds of active ingredients (except gypsum) in XFBDG according to the TCMSP database, including 12 kinds of Ephedra, nine kinds of bitter apricot seed, six kinds of the seed of Job's tears, two kinds of Rhizoma Atractylodis, six kinds of patchouli, 17 kinds of sweet wormwood herb, seven kinds of *Polygonum cuspidatum*, eight kinds of European verbena herb, one kind of reed rhizome, five kinds of *Lepidium* seed, seven kinds of pomelo peel, and 81 kinds of root of Ural licorice (Table 1). The main component of gypsum is $CaSO_4$, and 249 kinds of effective component target proteins were obtained after protein prediction and standardized treatment.

3.2. Intersection Target of "Intestinal Flora Disorder-Related Protein" and "Target Protein of XFBDG." 406 proteins related to intestinal flora disorder were obtained from the GeneCards database, and 57 proteins were obtained after the intersections with 249 drug target proteins (Figure 1).

3.3. GO and KEGG Enrichment Analysis. The results of GO and KEGG enrichment analysis showed the following: GO functional enrichment analysis revealed a total of 2001 functional items (Figure 2), among which there were (1) 1829 BP, mainly including response to the drug, cellular response to chemical stress, response to the metal ion, response to oxidative stress, response to lipopolysaccharide, and response to molecule of bacterial origin; (2) 30 CC, mainly relating to transcription regulator complex, vesicle lumen, and membrane raft; and (3) 142 MF, mainly involving RNA polymerase II-specific DNA-binding transcription factor binding, DNA-binding transcription factor binding, and cytokine activity. The KEGG pathway enrichment analysis revealed a total of 152 signaling pathways (Figure 3). IL-17 signaling pathway [11], TNF signaling pathway [12], and Th17 cell differentiation [13] have the closest relation with intestinal microflora disorder. The interaction network of pathway-enriched proteins was constructed (Figure 4(a)) in which the yellow node represents core proteins and the red node represents related proteins, the blue triangle represents the pathways related to intestinal flora disorder, the red circular node represents the general enrichment proteins, and the yellow circular node represents core enrichment protein in the pathway-target topology analysis network (Figure 4(b)). Therefore, IFNG, IL4, PTGS2, JUN, IL1B, IL6, TNF, RELA, and CASP3 appear to play key roles in regulating the IL-17, TNF, and Th17 cell differentiation signaling pathways.

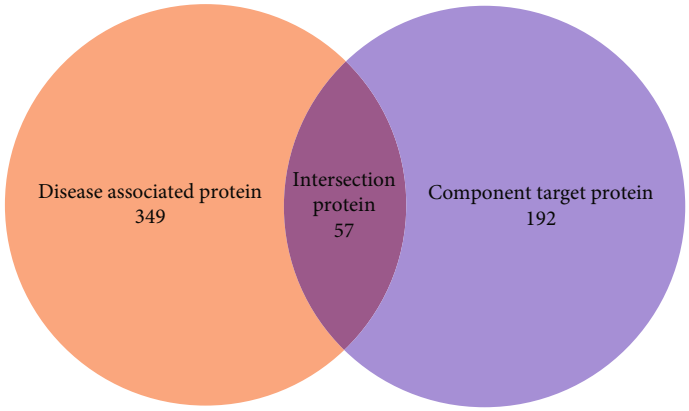

Figure 1: Venn diagram of intersection targets of XFBDG and related protein of intestinal flora disorder.

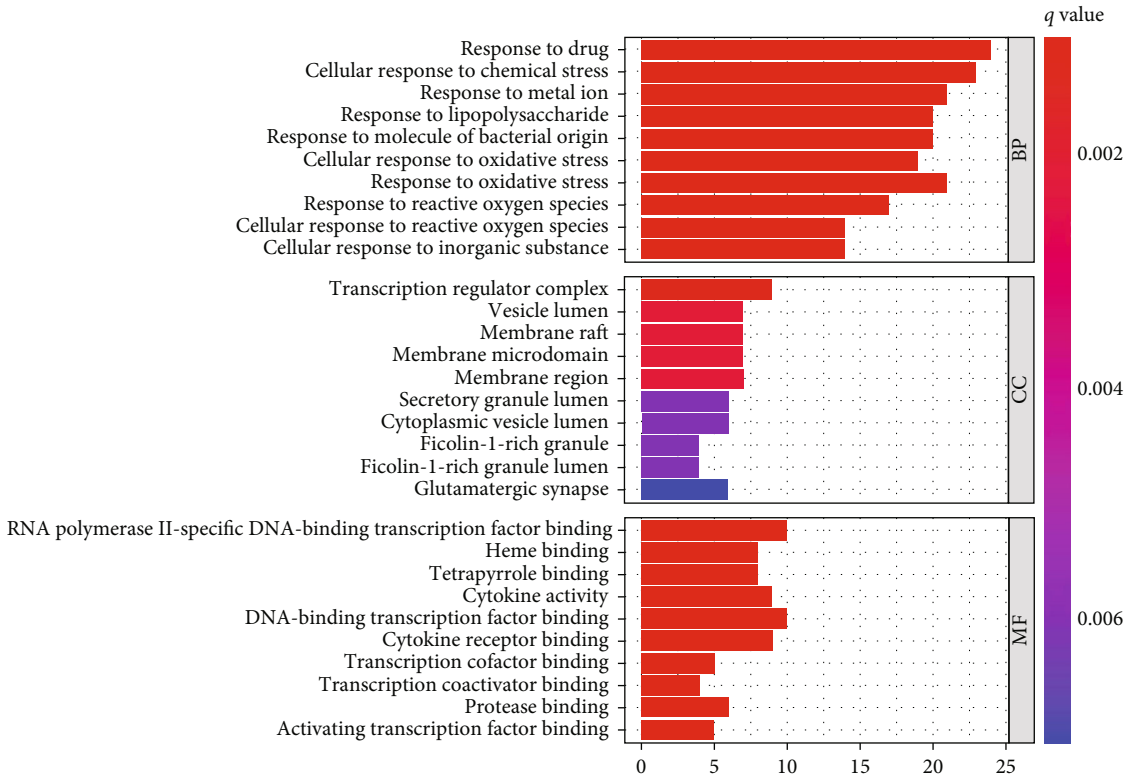

Figure 2: GO enrichment analysis of intersection targets of XFBDG and intestinal flora disorder.

3.4. Network Construction of Drug Component-Target Protein. The results of the drug component-target protein topological analysis network (Figure 5) show that the network contains 151 nodes and 307 connection lines. In the figure, the inside matrix represents the drug effective components: cyan is the root of Chinese licorice, dark green is the seed of Job's tears, orange is sweet wormwood herb, gray is patchouli, brown is Ephedra, blue is *Lepidium* seed, blue gray is bitter apricot seed, purple is *Polygonum cuspidatum*, pink is pomelo peel, and light blue is Rhizoma Atractylodis. Multicolored nodes represent the components that drugs commonly have, while circular structures represent the pathway-enriched proteins. For example, red is the general enriched protein, and yellow is the core enriched protein. The results show that the main components of this prescription are quercetin, luteolin, wogonin, kaempferol, and irisolidone, and PTGS2 is the top one strongly regulated by drugs among the core proteins.

3.5. Molecular Docking between the Core Target and the Drug Effective Ingredient. The affinity between receptor and ligand that goes lower than -5 kJ·mol^{-1} indicates that the receptor and ligand have a good binding ability [14]. The docking accuracy between the core target protein and corresponding main components was verified by the molecular docking experiment. The affinity between the target protein and the corresponding compound was <-5 kJ·mol^{-1} (Table 2), and the molecular docking pattern constructed

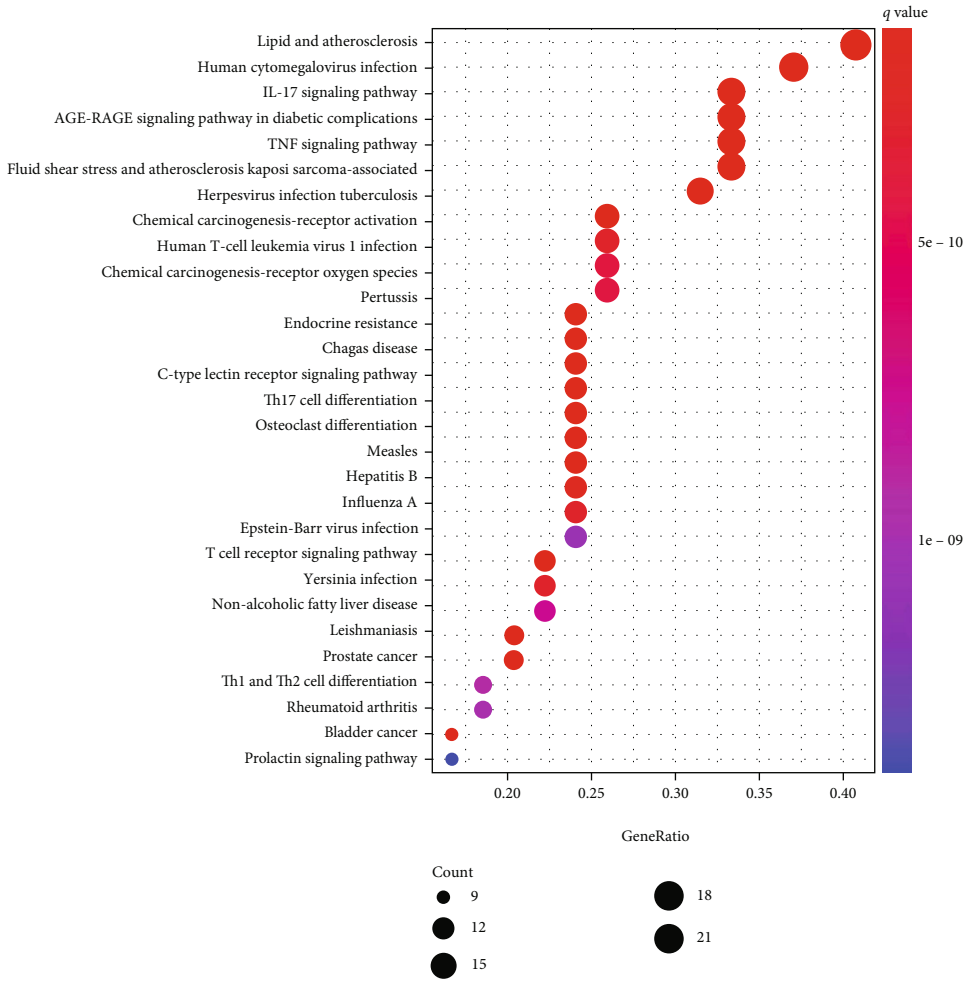

Figure 3: KEGG enrichment analysis of intersection targets of XFBDG and intestinal flora disorder.

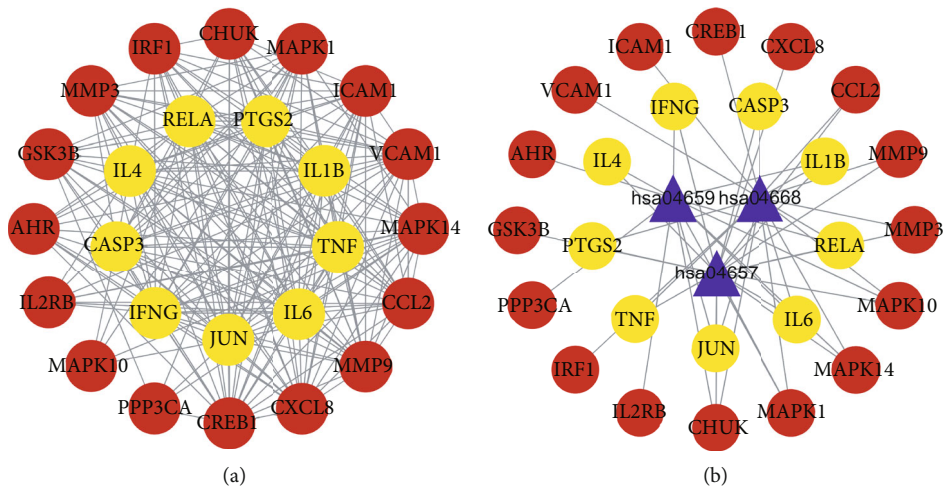

Figure 4: (a) represents the interaction network of pathway-enriched proteins, and (b) represents the pathway-target topology analysis.

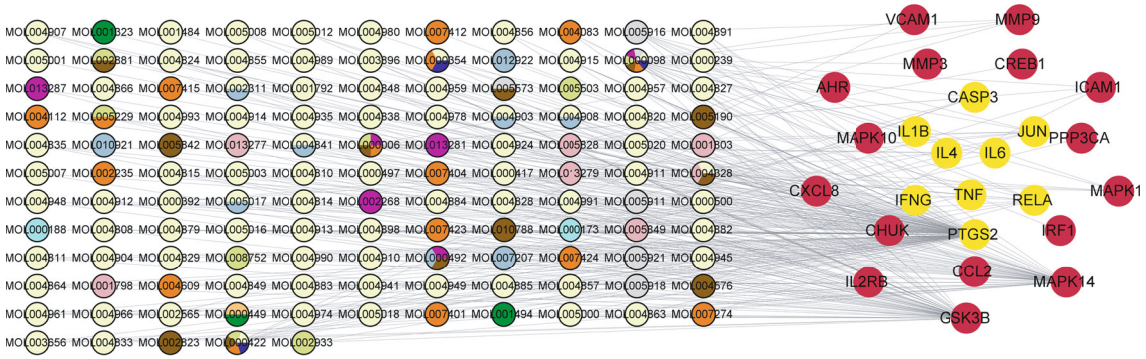

Figure 5: Component-target topology analysis.

Table 2: Molecular docking data of component-target.

Target protein	Affinity/(kJ·mol^{-1})				
	Quercetin	Luteolin	Wogonin	Kaempferol	Irisolidone
IFNG	-7.3	-7.1	—	—	—
IL4	—	-7.5	—	—	—
PTGS2	-9.6	—	—	-9.2	—
JUN	-8.2	-8.1	—	-8.1	-8.3
IL1B	-7.3	—	—	—	-6.5
IL6	-6.9	-7.1	-6.4	—	—
RELA	-7.7	-7.7	-7.5	-7.3	-7
TNF	-8.8	-8.6	-6.3	-8.6	-8.3
CASP3	-7.9	-7.8	-7.4	-7.7	—

with the target protein and the compound with the strongest affinity (Figure 6) showed that there was a good binding ability between the drug component and the target.

4. Discussion

XFBDG is a compound prescription of MXSGD, MXYGD, TLDZXFD, and QJWJD and works by ventilating the lungs to eliminate dampness, clearing heat to expel pathogenic factors from the exterior, removing heat from the lung, and detoxifying. According to TCM, "the lungs and the large intestine are intertwined in a mutual relationship," which means that both organs interact with and are influenced by each other, both physiologically and pathologically. Intestinal flora not only affects the maturation and development of the host immune system but also affects the stability of the host metabolic homeostasis through the cross-communication of microbial metabolites or cometabolites. Our study suggests that alteration of microbiological flora could be one of the manifestations of "pulmonary and intestinal disease." Modern medicine believes that various respiratory diseases can be prevented by regulating intestinal flora and immunity system, suggesting that the "gut-lung" axis could be the bridge between the lung and large intestine. MXSGD could alleviate bronchial asthma by improving the intestinal flora and has noticeable efficacy in the treatment of pediatric mycoplasma pneumonia with azithromycin. QJWJD has similar immune effects on the decomposition of intestinal flora and filamentous bacteria. Using network pharmacology, it has been possible to make multiple clarifications regarding the action mechanism of drugs, and molecular docking has helped calculate the affinity between receptors and ligands. Therefore, with the help of network pharmacology and molecular docking methods, this study preliminarily explored the specific mechanisms such as components, targets, and pathways involved in the treatment of intestinal flora disorders by XFBDG.

Based on the GO functional enrichment analysis, it was found that XFBDG has a therapeutic effect on intestinal flora disorder involving the regulation of response to oxidative stress, response to the drug, cellular response to chemical stress, and other functions. For instance, response to oxidative stress refers to the imbalance in the generation and metabolism of oxygen free radicals in tissues. This can cause oxidative damage induced by the accumulation of reactive oxygen species (ROS) and the ratio disproportion between antioxidant enzymes and lipid peroxides. ROS can activate/inhibit a series of signaling pathways which, in turn, can cause pathological changes such as the proliferation and migration of pulmonary vascular smooth muscle cells (PASMC), pulmonary endothelial cells (PAEC) disorder, *in situ* thrombosis, inflammation, pulmonary vascular remodeling, vasoconstriction response, and extracellular matrix deposition [15, 16]. According to the KEGG pathway enrichment analysis, XFBDG has proven effective in inhibiting the development of intestinal flora disorder by regulating

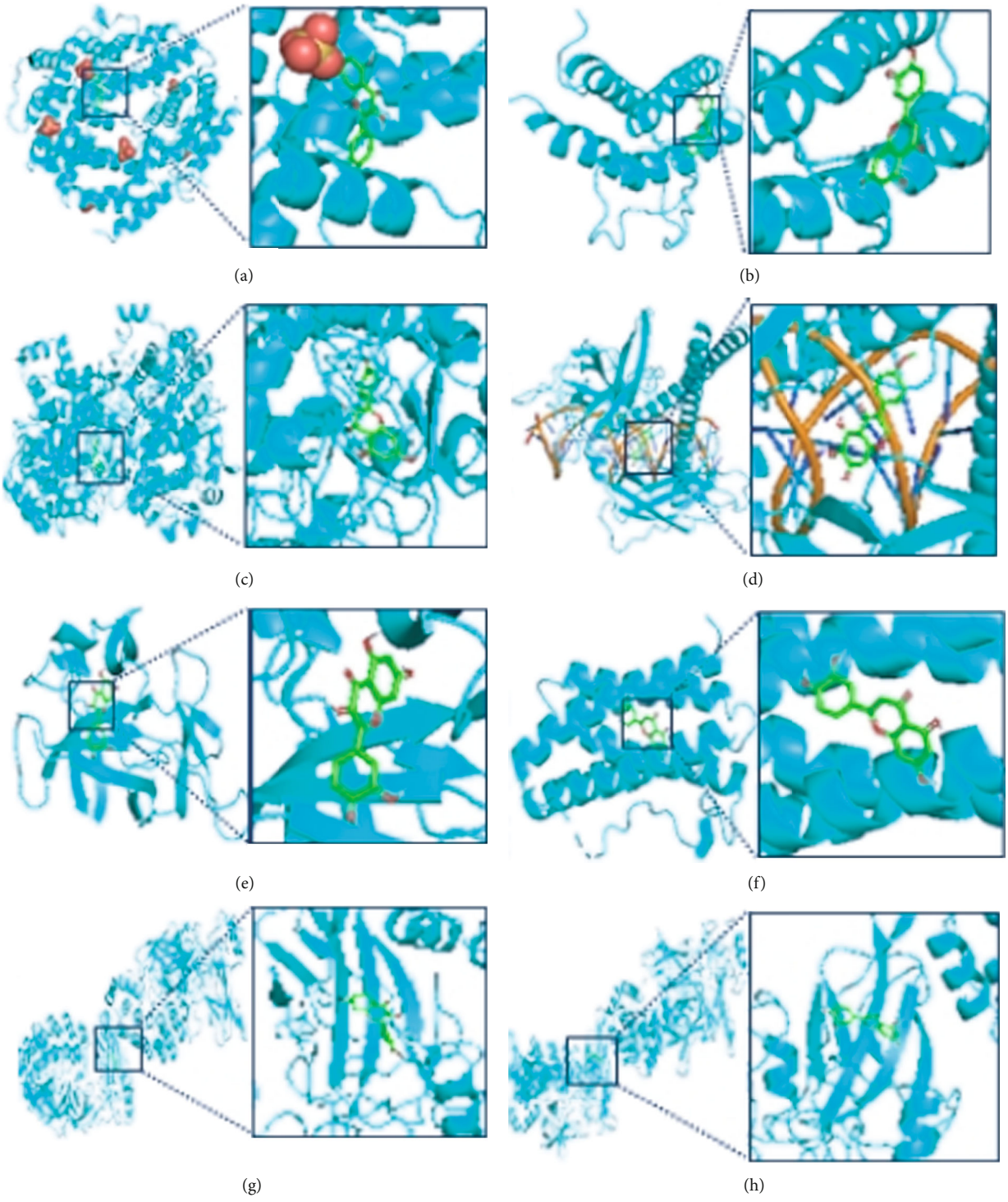

Figure 6: Continued.

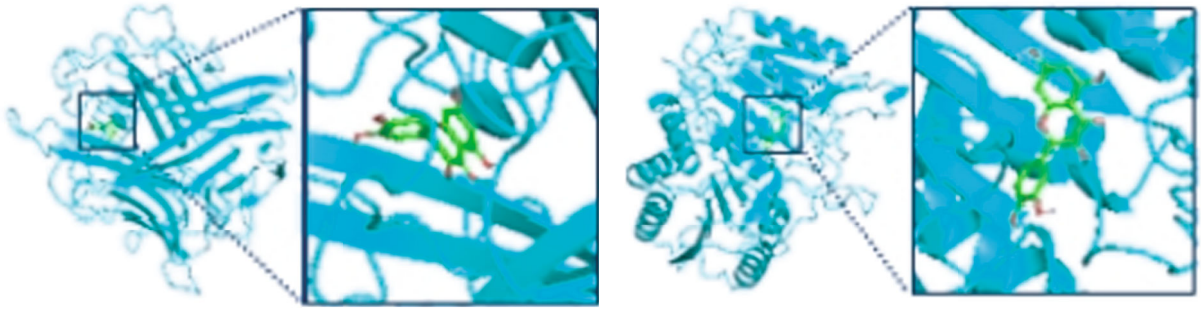

(i) (j)

Figure 6: Molecular docking pattern diagram. (a) is IFNG and Quercetin, (b) is IL4 and luteolin, (c) is PTGS2 and quercetin, (d) is JUN and irisolidone, (e) is IL1B and quercetin, (f) is IL6 and luteolin, (g) is RELA and quercetin, (h) is RELA and luteolin, (i) is TNF and quercetin, and (j) is CASP3 and quercetin.

the IL-17, TNF, and Th17 cell differentiation signaling pathways. Furthermore, stimulating the secretion of cytokines IL-17 can (i) increase the number of intestinal epithelium lymphocytes and enrich the availability and diversity of probiotics, (ii) lower the levels of pathogenic bacteria, (iii) enhance the intestinal mucosal immunity of rats, (iv) improve the intestinal inflammation and the intestinal flora disorders in barrier function and adjustment, and (v) especially promote the growth of beneficial intestinal flora, adjust the flora structure, and restore the intestinal immune function [11, 17, 18]. Hypoxia exposure can significantly aggravate the symptoms and pathological damage in rats. Downregulating the Th1 and Th17 responses in rats with colitis to affect the immune function and regulate Th17/Treg signaling pathway can both restore the homeostasis of intestinal flora in rats. Meanwhile, regulating the abundance, diversity, and composition of intestinal flora can also restore the balance of Th17/Treg to improve the survival status of rats [13, 18–20]. The growth and abundance of intestinal flora are correlated with the level of TNF-α. The stronger the expression of TNF-α, the larger the numbers of *Escherichia coli*, *Enterococcus faecalis*, and *Bacteroides fragilis* and the smaller the numbers of *Bifidobacterium* and *Lactobacillus*. Therefore, reducing the expression of proinflammatory factors can improve the intestinal flora of rats [12, 21–23].

The main components of XFBDG including quercetin, luteolin, and kaempferol are obtained through enriched core protein screening, pathway-target topology analysis, component-target topological analysis, and molecular docking; the above pathways are regulated by intervening core proteins such as IFNG, IL4, PTGS2, JUN, and IL1B. Modern pharmacological studies have shown that quercitrin is a member of the flavonoid family with antioxidant and anti-inflammatory effects and is also regarded as a prebiotic with antibacterial effects, which can significantly affect the intestinal environment and regulate intestinal flora. Flavonoid glycosides can be hydrolyzed by the intestinal flora, and quercetin can be transformed into corresponding aglycones under the metabolic action of human intestinal bacteria. Therefore, the content of flavonoid aglycone with strong anticomplement activity is significantly increased and thus can change the metabolic function of rat intestinal flora. In particular, the intestinal microbiota closely relates to human diseases (such as increasing the proportion of Clostridium and lactic acid bacteria and reducing the proportion of *E. coli*), affects the metabolic homeostasis of rat intestinal microbiota host, and helps to improve the enzyme system of human intestinal microbiota metabolism and response mechanism [24, 25]. Luteolin is a kind of flavonoid and studies about its effects on lipid metabolism disorder and intestinal flora composition in rats fed a high-fat diet shows that luteolin combined with metformin hydrochloride can decrease the proportion of Firmicute and Bacteroidetes (F/B), to increase the relative abundance of Lachnospiraceae, Helicobacteraceae, algae, and Peptococcaceae as well as alleviate lipid metabolism disorder and optimize the composition of intestinal flora in high-fat diet rats. In addition, luteolin can enhance the intestinal barrier by decreasing the level of reactive oxygen species (ROS), increasing the activity of superoxide dismutase (SOD) and glutathione (GSH), and inhibiting the secretion of proinflammatory cytokines [26, 27]. Kaempferol is a natural flavanol with multiple pharmacological activities. Metabolomic studies have shown that kaempferol treatment can significantly reverse the interference of energy production and metabolites that are involved in tryptophan, fatty acids, and secondary bile acids in the intestinal contents of rats, and can, to a large extent, restore the imbalance of intestinal flora and microbial metabolism of rats to achieve the regulation effects of anti-inflammatory and immune response [24, 28, 29]. Although this study only applies network pharmacology and molecular docking technology to analyze the capacity of drug active components in absorption and binding and have not considered the content and interaction of drug active components in the compound prescription, the results can still provide a general referential direction for clinical and experimental research.

5. Conclusion

XFBDG is advantageous in the treatment of intestinal flora disorder with multicomponents, multitargets, and multipathways. Using the network pharmacology method to analyze the molecular mechanism by which XFBDG can treat

intestinal flora disorder, this study found that the main mechanism is likely via quercetin, luteolin, kaempferol, and other active components that act on IFNG, IL4, PTGS2, JUN, IL1B, and other core proteins to regulate the IL-17, TNF, and Th17 cell differentiation signaling pathways. This ensures balance of the intestinal flora and microbial metabolism, which helps to further fulfill the functions of antioxidation, anti-inflammation, and immune response regulation.

Data Availability

The data is available and will be provided upon request to the corresponding authors.

Conflicts of Interest

The authors declare that they have no known competing financial interests or personal relationships that could have appeared to influence the work reported in this paper.

Authors' Contributions

Yaodong Miao, Zeyu Zhang, and Yaoyuan Liu contributed to writing of the original draft. Yaodong Miao, Rui Chen, and Fengwen Yang contributed to writing-review and editing. Junhua Zhang contributed to study conception and design, investigation, and supervision.

Acknowledgments

The authors greatly appreciate the financial support from Foundation of State Key Laboratory of Component-Based Chinese Medicine (Grant No. CBCM2020203), which ensured the accomplishment of the work.

References

[1] G. de Oliveira, C. Oliveira, C. F. Pinzan, L. V. V. de Salis, and C. R. B. Cardoso, "Microbiota modulation of the gut-lung axis in COVID-19," *Frontiers in Immunology*, vol. 12, article 635471, 2021.

[2] R. P. Dickson, B. H. Singer, M. W. Newstead et al., "Enrichment of the lung microbiome with gut bacteria in sepsis and the acute respiratory distress syndrome," *Nature Microbiology*, vol. 1, no. 10, p. 16113, 2016.

[3] J. Tang, L. Xu, Y. Zeng, and F. Gong, "Effect of gut microbiota on LPS-induced acute lung injury by regulating the TLR4/NF-kB signaling pathway," *International Immunopharmacology*, vol. 91, article 107272, 2021.

[4] G. Ranucci, V. Buccigrossi, M. B. D. Freitas, A. Guarino, and A. Giannattasio, "Early-life intestine microbiota and lung health in children," *Journal of Immunology Research*, vol. 2017, Article ID 8450496, 2017.

[5] Y. Li, F. Chu, P. Li et al., "Potential effect of _Maxing Shigan decoction_ against coronavirus disease 2019 (COVID-19) revealed by network pharmacology and experimental verification," *Journal of Ethnopharmacology*, vol. 271, article 113854, 2021.

[6] L. Li, F. G. Lu, and Q. H. He, "Efficacy of Maxing Shigan Decoction combined with Western medicine for pneumonia in children: a systematic review and meta-analysis," *Zhong Xi Yi Jie He Xue Bao*, vol. 7, no. 9, pp. 809–813, 2009.

[7] K. Atarashi, T. Tanoue, Y. Umesaki, and K. Honda, "Regulation of Th17 cell differentiation by intestinal commensal bacteria," *Beneficial Microbes*, vol. 1, no. 4, pp. 327–334, 2010.

[8] L. H. Cao, Y. Y. Zhao, J. X. Miao et al., "Effect of fresh Phragmitis Rhizoma on airway inflammation in chronic bronchitis based on TGF-β signaling pathway," *Zhongguo Zhong Yao Za Zhi*, vol. 46, no. 22, pp. 5887–5894, 2021.

[9] C. A. Lipinski, "Rule of five in 2015 and beyond: target and ligand structural limitations, ligand chemistry structure and drug discovery project decisions," *Advanced Drug Delivery Reviews*, vol. 101, pp. 34–41, 2016.

[10] C. A. Lipinski, "Lead- and drug-like compounds: the rule-of-five revolution," *Drug Discovery Today: Technologies*, vol. 1, no. 4, pp. 337–341, 2004.

[11] Q. Chen, R. Ren, Q. Zhang et al., "_Coptis chinensis_ Franch polysaccharides provide a dynamically regulation on intestinal microenvironment, based on the intestinal flora and mucosal immunity," *Journal of Ethnopharmacology*, vol. 267, article 113542, 2021.

[12] Z. M. Song, F. Liu, Y. M. Chen, Y. J. Liu, X. D. Wang, and S. Y. du, "CTGF-mediated ERK signaling pathway influences the inflammatory factors and intestinal flora in ulcerative colitis," *Biomedicine & Pharmacotherapy*, vol. 111, pp. 1429–1437, 2019.

[13] Y. G. Wang, Y. Gao, J. Feng, and Y. Q. Dou, "Effect of Modified Xijiao Dihuang Decoction (加味犀角地黄汤) on intestinal flora and Th17/Treg in rats with radiation enteritis," *Chinese Journal of Integrative Medicine*, vol. 27, no. 3, pp. 198–205, 2021.

[14] K. Y. Hsin, S. Ghosh, and H. Kitano, "Combining machine learning systems and multiple docking simulation packages to improve docking prediction reliability for network pharmacology," *PLoS One*, vol. 8, no. 12, article e83922, 2013.

[15] A. C. Racanelli, S. A. Kikkers, A. Choi, and S. M. Cloonan, "Autophagy and inflammation in chronic respiratory disease," *Autophagy*, vol. 14, no. 2, pp. 221–232, 2018.

[16] N. Ghasemzadeh, R. S. Patel, D. J. Eapen et al., "Oxidative stress is associated with increased pulmonary artery systolic pressure in humans," *Hypertension*, vol. 63, no. 6, pp. 1270–1275, 2014.

[17] C. W. Shi, M. Y. Cheng, X. Yang et al., "Probiotic lactobacillus rhamnosus GG promotes mouse gut microbiota diversity and T cell differentiation," *Frontiers in Microbiology*, vol. 11, article 607735, 2020.

[18] M. Yang, F. Li, R. Zhang et al., "Alteration of the intestinal microbial flora and the serum IL-17 level in patients with Graves' disease complicated with vitamin D deficiency," *International Archives of Allergy and Immunology*, vol. 183, no. 2, pp. 225–234, 2022.

[19] X. Su, X. Yin, Y. Liu et al., "Gut dysbiosis contributes to the imbalance of Treg and Th17 cells in Graves' disease patients by propionic Acid," *The Journal of Clinical Endocrinology and Metabolism*, vol. 105, no. 11, pp. 3526–3547, 2020.

[20] Q. Ji, Y. Zhang, Y. Zhou et al., "Effects of hypoxic exposure on immune responses of intestinal mucosa to _Citrobacter_ colitis in mice," *Biomedicine & Pharmacotherapy*, vol. 129, article 110477, 2020.

[21] Y. Zhu, Y. Li, M. Liu, X. Hu, and H. Zhu, "Guizhi Fuling Wan, Chinese herbal medicine, ameliorates insulin sensitivity in

pcos model rats with insulin resistance via remodeling intestinal homeostasis," *Front Endocrinol (Lausanne)*, vol. 11, p. 575, 2020.

[22] J. Lu, S. S. Ma, W. Y. Zhang, and J. P. Duan, "Changes in peripheral blood inflammatory factors (TNF-α and IL-6) and intestinal flora in AIDS and HIV-positive individuals," *Journal of Zhejiang University. Science. B*, vol. 20, no. 10, pp. 793–802, 2019.

[23] Y. Zhong, C. Zheng, J. H. Zheng, and S. C. Xu, "The relationship between intestinal flora changes and osteoporosis in rats with inflammatory bowel disease and the improvement effect of probiotics," *European Review for Medical and Pharmacological Sciences*, vol. 24, no. 10, pp. 5697–5702, 2020.

[24] X. L. Qin, H. Y. Sun, W. Yang et al., "Analysis of metabolites of quercitrin in rat intestinal flora by using UPLC-ESI-Q-TOF-MS/MS," *Zhongguo Zhong Yao Za Zhi*, vol. 42, no. 2, pp. 357–362, 2017.

[25] X. Jin, Y. Lu, S. Chen, and D. Chen, "UPLC-MS identification and anticomplement activity of the metabolites of _Sophora tonkinensis_ flavonoids treated with human intestinal bacteria," *Journal of Pharmaceutical and Biomedical Analysis*, vol. 184, article 113176, 2020.

[26] X. Ge, C. Wang, H. Chen et al., "Luteolin cooperated with metformin hydrochloride alleviates lipid metabolism disorders and optimizes intestinal flora compositions of high-fat diet mice," *Food & Function*, vol. 11, no. 11, pp. 10033–10046, 2020.

[27] J. Yuan, S. Che, Z. Ruan, L. Song, R. Tang, and L. Zhang, "Regulatory effects of flavonoids luteolin on BDE-209-induced intestinal epithelial barrier damage in Caco-2 cell monolayer model," *Food and Chemical Toxicology*, vol. 150, article 112098, 2021.

[28] L. X. Aa, F. Fei, Q. Qi et al., "Rebalancing of the gut flora and microbial metabolism is responsible for the anti-arthritis effect of kaempferol," *Acta Pharmacologica Sinica*, vol. 41, no. 1, pp. 73–81, 2020.

[29] L. Xin, X. H. Liu, J. Yang et al., "The intestinal absorption properties of flavonoids inHippophaë rhamnoidesextracts by anin situsingle-pass intestinal perfusion model," *Journal of Asian Natural Products Research*, vol. 21, no. 1, pp. 62–75, 2019.